

Galactic kinematics of various stellar types

CHARLES R. COWLEY¹ AND ROBERT E. STENCEL^{2,*}

¹*Department of Astronomy, University of Michigan, 1085 S. University, Ann Arbor, MI 48109-1107
orcid:0000-0001-9837-3662
e-mail: cowley@umich.edu*

²*Chamberlin Observatory, University of Denver, 2930 E Warren Ave., Denver, CO 80210, USA,
orcid:0000-0001-8217-9435
e-mails: robert.stencel@du.edu
restence@umich.edu*

ABSTRACT

We compare and contrast the kinematics of various classes of stars, both normal (with MK types) and peculiar. Numerous plots show the differences in spatial and velocity distributions as well as distributions in kinetic energy vs. angular momentum (KE vs. L_Z) space. In the latter plots, young, thin disk stars on nearly circular orbits cling to the left edge of a “solar parabola” while older objects on elliptical orbits fill the central parabolic region. Some of the young Wolf-Rayet stars violate this trend due to smaller semi-major axes than the Sun or orbital eccentricities. Deviation of the vertex of the velocity ellipsoid is discussed as an indication of population and youth, with an emphasis on Ap, Bp, Am, Fm, Herbig AeBe, and λ Bootis stars. Both the vertex deviation and phase space distribution provide useful insights.

Keywords: stars: normal – stars: solar-type – stars: kinematics and dynamics – stars: Wolf-Rayet – stars: chemically peculiar – stars: abundances – Galaxy: solar neighborhood –

1. INTRODUCTION

In this paper we examine the kinematical properties of groups of stars that are distinguished by their spectral peculiarities. Data in the Simbad and Gaia data bases¹ allow calculation in physical (X, Y, Z) and velocity space (U, V, W) with respect to the local standard of rest (LSR), here assumed to be 8.5, 13.58, and 6.49 km s⁻¹. Numerical values for the latter were taken from PyAstronomy² The present work uses a right-handed coordinate system in which X and U point to the Galactic center, while Y and V are in the direction of Galactic rotation.

We show plots of Y vs. X , distributions in the Galactic plane for various categories of stars. The present work emphasizes different peculiar types rather than subclasses of spectral types (e.g. G0 V, G2 V, etc.). The area covered by the stars generally reflect the intrinsic

brightness of the sample, such as O-stars vs G-dwarfs, and the area of the sky covered by the relevant survey. The plots may show associations with young clusters or spiral arms, or be associated with the sky fraction covered and/or the nature of the program from which the star sample was obtained. In the case of G-dwarf solar twins, the spatial plots are of the solar neighborhood because the relevant survey was a search for extrasolar planets, best studied in nearby objects (Bedell, et al. 2018)[henceforth BD18].

Plots of V vs. U for O-, Wolf-Rayet (henceforth, WR), and Herbig AeBe are dynamically unrelaxed, and show the influence of clusters and spiral arms. For later spectral types, A, B, and especially F and G, the U vs. V plots are more ordered (relaxed) and may be considered to be a projection of a velocity ellipsoid. This concept was introduced by Schwarzschild (1907), and widely investigated over the years.

A fine introduction of the velocity ellipsoid and the related phenomenon of *vertex deviation* is in Mihalas & Routly (1968). Since the mid 20th Century, vertex deviation has been discussed in relation to stellar populations (Vyssotsky 1957). The *angle* of deviation is

* Department Astronomy, Univ. Michigan, Ann Arbor

¹ See Sec. Data for detailed references.

² Code site: <https://tinyurl.com/zkwzvrt8> or <https://github.com/sczesla/PyAstronomy>

measured clockwise from the direction of Galactic rotation, and *tends to decline with increasing age* (Binney & Merrifield 1998) – see p. 631. Gomez et al. (1990) showed that the kinematics and vertex deviation of the local Population I dwarf stars (B5 V-F5 V), were related to age (Sun et al. 2023). We note vertex deviations in Sec. ApBp-stars, AmFm-stars and lamBoo-stars. However, attempts to measure relative ages from the angles of deviation have proven unsatisfactory. Some unweighted least squares fits to the points in UV space give angles that are not consistent with eyeball fits, probably because of outliers. We therefore show the relevant plots, and leave further quantitative evaluations to future work.

We also show plots in KE vs. L_Z space, where the coordinates are stellar kinetic energies (KE) and the z-component of the angular momentum L_Z , both defined per appropriate unit mass. For the plots, we take the origin of the coordinate system to be the center of the Galaxy. For these coordinates it is only necessary to substitute $X = X - R_c$, for the X-coordinate, and $V = V + V_c$, where V_c is the circular velocity at the Local Standard of Rest (LSR). We use 8 kpc for R_c .

In the KE vs. L_Z space plots, the solar X is -8 kpc. If we assume all of the kinetic energy is entirely due to a the circular velocity V_c km/s, then

$$KE = \frac{1}{2} V_c^2. \quad (1)$$

For a circular orbit, the Z -component of the angular momentum, $L_z = XV - YU$ and $L_z = R_c \times V_c$. It is common in calculations of this type to assume unit mass.

From these simple relations we obtain a parabola

$$KE = \frac{1}{(2 \cdot R_c^2)} \times L_z^2. \quad (2)$$

This defines the *solar parabola* to which we shall henceforth refer. Note that our KE vs. L_Z plot is qualitatively different from energy vs. L_Z plots where the energy is the total, kinetic plus potential energy. The Galactic potential energy may dominate the kinetic, so a plot of total energy vs. L_Z can be qualitatively different from one where only the kinetic energy is used. We also neglect any influence of the Galactic bar (Moreno et al. 2015).

The Solar twins of BD18 and Spina et al. (2018) are often used here as representative, thin disk stars. Indeed, most of our stars are thin-disk Population I and generally confined to the Galactic plane. We show this explicitly for the WR and Herbig AeBe stars, but in the summary section (below), we give the average absolute value of the coordinate Z for all of the data sets.

The Ap, Bp, Fp, HgMn, and λ Bootis stars are subclasses of CP or chemically peculiar stars of the upper main sequence (Preston 1974) and (Gray & Corbally 2009). Their peculiar compositions are currently thought to originate primarily from endogenous elemental separations due to diffusion under radiation pressure (Michaud 1970) with possible mass loss. A comprehensive review is by Michaud et al. (2015).

1.1. Radial velocities and parallaxes

Many radial velocities are missing from the Gaia DR3 for the O- and WR stars and those that are present are typically unreliable. Useful lines are often broader than in later types, and often partially or wholly in emission. In some of the more distant stars, there can be perturbations from interstellar material. For that reason for O- and WR stars we have used estimates based on the transverse velocities in right ascension and declination; We assumed that the radial velocity is equal to the mean of the two transverse velocities, with alternating positive and negative values. We designate these as “the estimated RVs”. We note but have not implemented statistical ways of estimating the radial velocities (Naik & Widmark 2023), which require knowledge of stars near the O- or Wolf Rayet star. It is beyond the scope of the present work to obtain such data. As an alternative, we have calculated the distributions for A and F stars (which have good radial velocities) in UV space using both the spectroscopic and estimated radial velocities. The general distribution of points in both cases were quite similar.

Parallax errors are of primary concern. Errors of proper motion may make minor distortions in our plots but do not lead to serious mistakes such as giving unrealistic distances. We follow Plotnikova et al. (2023) who considered four different methods obtaining the best parallaxes from Gaia, and adopted those coming directly from Gaia DR3.

We considered a sample of Gaia DR3 Galactic O-Star Catalogue (GOSC) of Maiz Apellaniz et al. (2004) O-stars with small parallaxes ≤ 0.2 milliarcsec (mas). While there was considerable scatter, the parallax errors averaged roughly 0.1 times the the parallaxes. We also considered Gaia DR3 parallax over error vs. parallax. Again, there was is considerable scatter, showing a parallax over error value of 5 was obtained for parallax values of 0.08 to 0.1 mas. We have chosen the more conservative value and excluded all stars with parallax values less than 0.1 mas for all sets of stars in the present study.

For the WR stars we used distances estimated by P. Crowther (private communication) and considered

“good”. We did not consider his higher and lower distance estimates. Bayesian re-considerations of this point are not likely to improve on these estimates until alternate methods of radial velocity determination are found.

2. THE KINEMATICS OF GROUPS OF STARS

2.1. *O-stars*

We discuss 354 O-stars of all subclasses from the Galactic O-Star Catalogue (GOSC) of [Maiz Apellaniz et al. \(2004\)](#). Fig. 1A,B show that the GOSC O-stars are distributed far more widely in space than the solar twins of BD18 (merged green squares) which are all contained within a radius of about 100 pc. This is expected, as the BD18 twins contain only dwarfs chosen in planet searches, while the GOSC O-stars contain giants as well as dwarfs.

In (UV) velocity space (Fig.1C), both the O-star and solar twin motions fall mostly within a circle with 100 km/s radius shown. The O-stars show grouping in both physical and velocity space suggestive of clusters or spiral arms. The U and V points would be placed somewhat differently if actual rather than estimated radial velocities were used.

For the KE vs. L_Z space plot (Fig.1D) we again used radial velocity estimates based on the tangential motions. Because our X is zero for the center of the Galaxy and negative 8 kpc for the solar neighborhood, L_z is a large negative number for stars on prograde orbits (positive V). The BD18 solar twins are plotted as green squares while the GOSC O-stars are black, filled circles. Generally, young stellar populations cling to the parabola as do most of the solar twins.

Stars may fall into the interior of the solar parabola for various reasons. They may be on elliptical orbits or have circular orbits with radii less than that of the Sun. Very metal poor stars typically have elliptical and sometimes retrograde orbits as they belong to an old population.

Two high outliers near the center of the KE vs. L_Z plot are HD 157857, an O6.5 II(f) (upper left), and CD -26 5136 (lower right), a Blue Supergiant O 6.5 Iabf, according to Simbad.

2.2. *Wolf-Rayet (WR) stars*

The WR stars are a heterogeneous group of evolved massive stars. Most show strong emission lines of either nitrogen (WN stars) or carbon (WC stars). For a more detailed description of WR types see [Crowther \(2007\)](#). Fig. 2A shows the distribution in physical space of WR stars from the catalogue of Paul Crowther and colleagues

([Rosslowe & Crowther 2015a](#)), henceforth CCat (see also [Rosslowe & Crowther \(2015b\)](#); [Crowther \(2007\)](#)).³

The distances are from a private communication kindly sent by Paul Crowther. Only values which he considered good estimates were plotted. We used a crude classification where the red plus signs are from stars with the letter ‘C’ in the CCat classification, while blue triangles are for stars with ‘N’. Neither subtype shows a clear preference for a particular area of physical space.

The Galactic WR stars are clumped at a distance from the Galactic center that is somewhat less than that of the Sun, and they spread in the Y-direction—that of Galactic rotation. Fig. 2A may be compared with the plot in a recent paper by [Neugent & Massey \(2023\)](#) giving positions of N- and C-subtype WR stars in the Andromeda galaxy. Their Fig. 1 shows an elliptical ring of N and C WR types in about the same ratio as in our sample: C/N = 0.70, 0.63 (Galaxy, Andromeda). The WR stars in our Fig. 2A might represent a fraction of a similar ring in our own Galaxy.

Our results for the distribution of WR stars in (Galactic) physical space is very similar to those of [Rustamov & Abdulkarimova \(2023\)](#), who used a somewhat larger sample of WR stars.

Fig. 2C shows the WR stars in velocity space. The dispersion in velocities of the WR stars is significantly larger than that of the solar twins which would fall mostly within a 63 km/s circle. (see Fig. 2C) The WC and WN stars are intermixed. The magnitude and spread of the WR velocities is surprisingly large for a population of young stars. We note the significant, non-symmetric structure of the velocities, details of which are affected by the radial velocity approximations.

Fig. 2B shows the distribution of WR stars in the vertical direction and shows the concentration to the Galactic plane with the southern hemisphere somewhat more populated. The vertical envelope is similar to the ± 250 pc discussed by [Rustamov & Abdulkarimova \(2023\)](#). If we assume a lifetime of 1 Myr for a WR star at 240 km/s (see Fig. 2C), the star could travel 250 pc in about 1 Myr, (using 1 km/s = 1 pc in 10^6 years). This is the same order of magnitude as the estimate of a representative WR evolutionary phase ([Rosslowe & Crowther 2015a](#)).

A plot of KE vs. L_Z (Fig. 2D) gives additional perspective. A sizable fraction of the stars cling to or are near the negative branch of the solar parabola, where young stars reside. There is some scatter, even to positive L_Z , implying retrograde orbits. Such orbits are

³ <https://pacrowther.staff.shef.ac.uk/WRcat/>

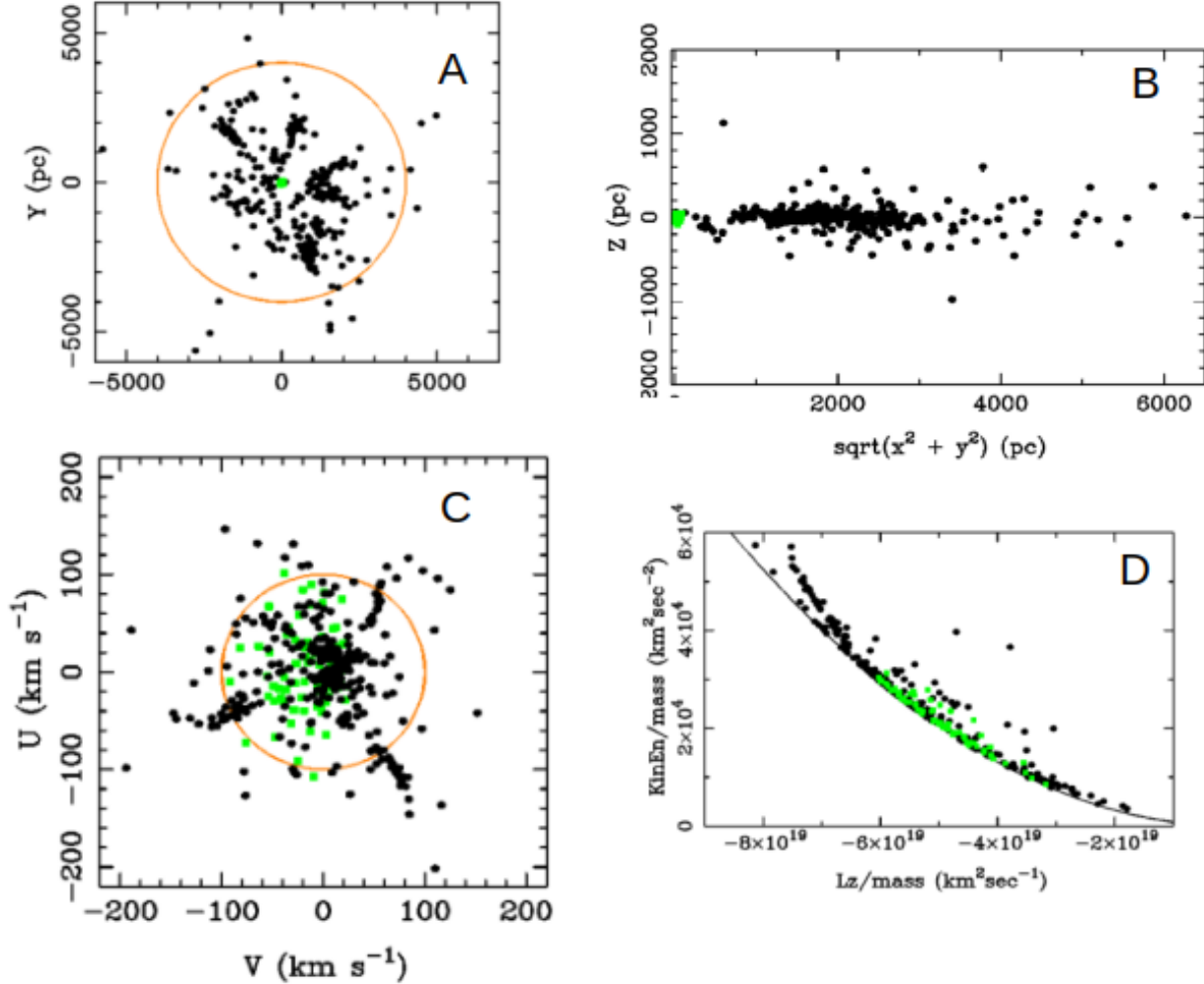


Figure 1. A. O star distribution in physical space from the GOSC Star Catalogue (Maiz Apellaniz et al. 2004). The G-dwarf, BD18 solar twins (merged green squares) are at the center of the plot and present a strong contrast. The orange circle is 4 kpc in radius. B. Z-axis distribution. C. The distribution of (GOSC) Ostars in velocity space (black filled circles) is only a little greater than that of of BD18 solar twins in green squares, in contrast to the X Y plot for physical space. Both sets of stars are in or near the 100 km/s orange circle. D. O stars of all types (black filled circles) from the GOSC catalogue are plotted in KE vs LZ space. Compare these with the BD18 sample.

typical of some very old, metal-poor dwarfs (Moreno et al. 2015; Cowley & Stencel 2023) and Table 1. Binary ejection may be responsible for some of the unusual velocities, which are difficult to understand for young WR stars. Some of the scatter to higher L_Z and KE is surely due to radial velocity estimates. The WR stars with the largest (positive) values of L_Z are: WR 29, WR 30a, and WR 61. We find no indication from Simbad or CCat that would explain their unusual L_z values.

An older catalogue by van der Hucht (2001) shows some WR stars lifting off the parabola, but shows no points in the positive (retrograde) L_z side.

2.3. Mercury-Manganese (HgMn) stars

HgMn stars are chemically peculiar, mostly B dwarfs, with weak or no measurable magnetic fields. Ghazaryan & Alecian (2016) describe the properties of this class and present a catalogue of abundances for 81 of these stars. They can have unbelievably bizarre abundances of heavy elements, such as a million times solar for mercury. A few of these stars show puzzling isotopic excesses of the rare ^{48}Ca (Castelli & Hubrig 2004). While the HgMn stars may also be considered Bp, only one of the 81 stars are in the set of ApBp stars of Section 2.5. This is because the HgMn types were nearly impossible to

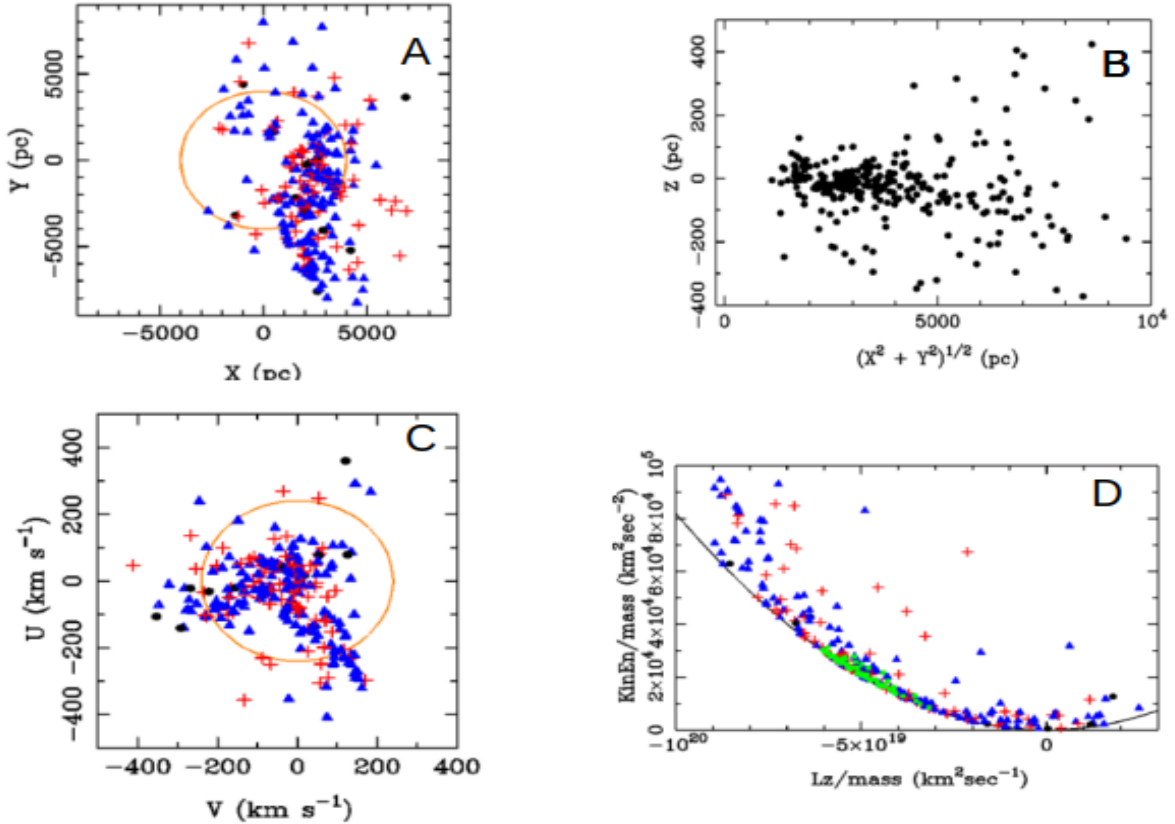


Figure 2. A. X and Y positions in the Galactic plane of WN (blue triangles) and WC (red plus signs) stars from CCat. The N- and C-types are intermixed. WR stars that are neither N nor C are plotted as black filled circles. The orange circle is 4 kpc in radius. B. WR stars from CCat showing the vertical (Z) direction. The envelope is similar to the 250 pc discussed by Rustamov & Abdulkarimova (2023). C. WR stars from CCat in velocity space. Symbols and colors are as before. The orange circle is at 240 km/s. D. KE vs. LZ plot of WN (blue triangles) and WC (red plus signs) stars. BD18 twins are green squares.

detect at the resolution of the Houk-Michigan (Houk & Swift 2000) spectra. We therefore discuss them as a separate class. Fig. 3AB shows the distribution in physical space of the 264 stars from Chojnowski et al. (2020) survey.

In Fig. 3C, we plot the Chojnowski et al. (2020) stars in velocity space. They are nearly all contained within the 63 km/s circle of low velocity stars.⁴ Indeed, their scatter is tighter than that of the BD18 solar twins. This should be contrasted with the wide distribution of the HgMn stars in physical space (XY) where HgMn stars scatter beyond one kpc. This broad scatter, surely, is only partially due to the great depth of the Chojnowski

et al. (2020) survey. The BD18 stars are all within 100 pc of the sun.

These HgMn stars are shown in Fig. 3D in KE vs. L_Z space. One of the modest outliers, 38 Dra, is noted in Simbad as a high proper motion star. Another, HD 53004 is described in Simbad as an eclipsing binary.

2.4. Herbig AeBe stars

We examine the kinematics of 215 Herbig AeBe stars from the study by Vioque et al. (2018). Herbig stars (Waters & Waelkens 1998)[henceforth, Herbig] may be considered more massive (2-10 M_{\odot}) analogues of the pre-main sequence T-Tauri stars. They are distinguished from the Ap, Am, and Bp types discussed below by their emission lines and infrared excesses which originate from their star-forming envelopes. They have a wide distribution in physical space as shown by Fig. 4AB with a clear preference for the direction of the Galactic center (positive X).

⁴ Near the middle of the 20th century, velocities in the mid 60's (km/s) were cited by Oort (1930) as a limit between low and high velocity stars—6 km/s became a favorite value. See also Chandrasekhar (1960)

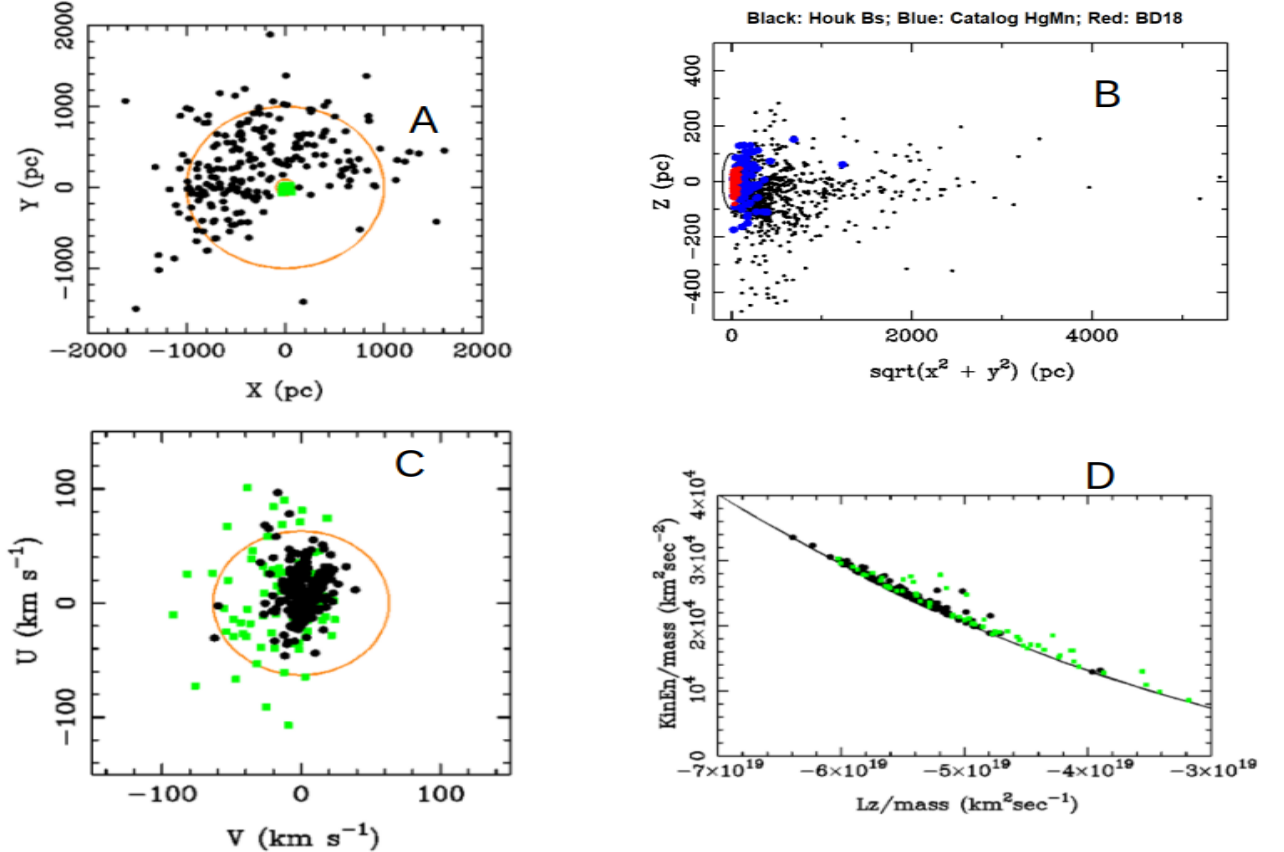


Figure 3. A. HgMn stars in physical space from Chojnowski et al. (2020) (black filled circles). The BD18 solar twins (green squares) are shown for perspective. The inner orange circle has a radius of 100 pc, the outer circle 1000 pc. The distribution is asymmetrical because of the sky survey coverage. B. Z axis locations with respect to galactocentric distance. C. HgMn stars in velocity space from Chojnowski et al. (2020), i.e. black filled circles. The BD18 solar twins (green squares) are shown for comparison. The circle has a radius of 63 km/s. D. HgMn stars in KE vs LZ space (black filled circles). The green squares are BD18 solar twins.

Among the Vioque et al. (2018) Herbig stars only about 30% have radial velocities in Gaia, so the remaining were estimated from the transverse velocities as was done for the O- and WR stars. Again the UV values are only approximate for those stars, but the overall character of the plots are not changed by the radial velocity estimates. The velocity space plot is shown in Fig. 4C. The distribution of velocities is similar to the BD18 solar twins, as was the case for the O-stars of Fig. 2.1.

In KE vs. L_Z space (Fig. 4D) the Herbig stars cling tightly to the left wing of the parabola, as would be expected for a very young population.

2.5. A_p , B_p types and superficially normal A and B dwarfs

Stars that are not specifically designated as peculiar have MK types assigned in the Houk-Michigan catalogues. We take them to be ‘superficially normal,’ or

simply ‘normal.’⁵ Plots in X vs Y of data from Houk & Swift (2000) are irregular in shape because of the partial sky coverage of the catalogues and are not shown. In velocity space, Fig. 5A, the points are distributed approximately circularly for A and B dwarfs. The ApBp types show a vertex deviation. The B dwarfs are largely obscured by the slightly wider A-dwarf distribution. The red points for ApBp stars show a vertex deviation.

These same stars are shown in the KE vs. L_Z space of Fig. 5B.

Five of the B-star outliers in Fig. 5B have some abnormalities: three are called *high proper motion*, another a double or multiple, and a fifth a hot subdwarf by Simbad.

⁵ Stellar spectroscopists have said that all stars are chemically peculiar if examined at high enough dispersion.

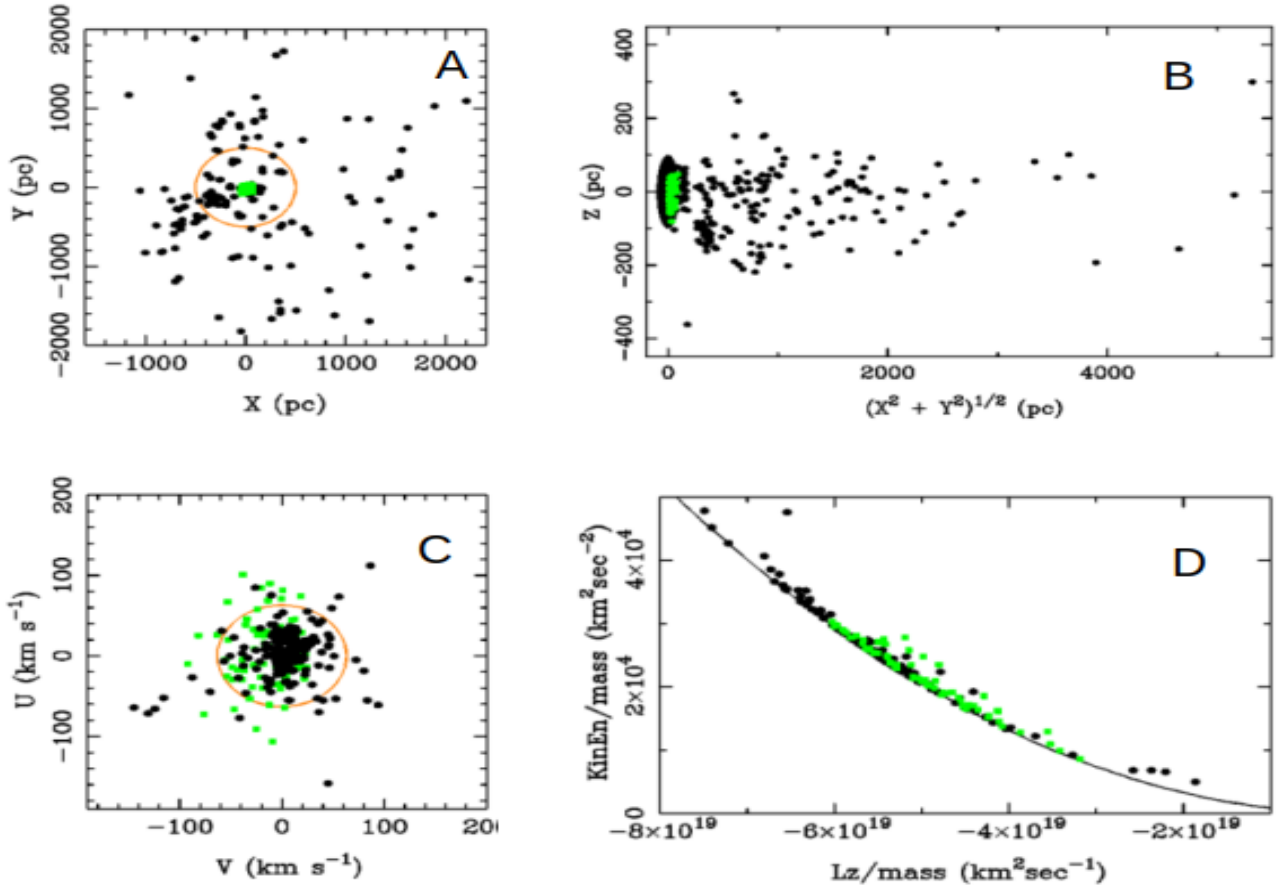


Figure 4. A. Herbig AeBe stars in physical space. The filled black circles are the Herbig AeBe stars from Vioque et al. (2018), the green squares within the orange circle of 500 pc are BD18 solar twins. B. The vertical extent of the Herbig AeBe stars (extra symbols as annotated). C. Herbig AeBe stars in velocity space (black). The circle is at 63 km/s. Unlike the spatial distribution, the velocities of the Herbig AeBe stars are similar to those of the solar twins. D. Herbig AeBe (black) and BD18 (green) stars in KE vs. LZ space. The plot is similar to other KE vs. LZ plots for young objects.

The behavior of the (red) crosses for the Ap and Bp stars is as expected if we attribute their peculiarities to endogenous diffusion and assume those effects diminish with age (Bailey et al. 2014). These young stars appear close to the $KE - L_Z$ parabola, and hardly stray into the region where older, metal-poor stars are found. The vertex deviation of Fig. 5A could indicate relative youth.

2.6. Am and Fm stars and normal A and F dwarfs from Houk-Michigan Catalogues

The physical space plot of F dwarfs and AmFm stars is also not shown because of the partial coverage of the Houk-Michigan catalogues. The velocity space plot, Fig.6 is similar to that of Fig. 5A, though slightly more compact. Note that the normal A dwarfs (blue triangles) are not plotted. The AmFm stars show a vertex deviation.

2.7. λ Bootis stars

Gray & Corbally (2002) describe the fascinating and chemically peculiar, upper main sequence stars, named after the prototype λ Bootis. Their abundance pattern is a depletion of elements with high condensation temperatures (Lodders 2003) while elements with low condensation temperatures have nearly solar abundances. This pattern is widely seen in a variety of astronomical settings from some Herbig AeBe stars (Folsom et al. 2012) and the interstellar medium (Venn & Lambert 1990).

The stars in the following plots were taken from Murphy et al. (2015) who provided a list of 212 possible λ Bootis stars. Only stars with “LamBoo” in the list were used here resulting in 90 stars. The dispersion in physical space of the λ Bootis stars 7A is noticeably larger than that of the BD18 solar twins because of their higher luminosities. In velocity space 7B, the relation is reversed, with the λ Boo stars more nearly equal to the Sun’s velocity.

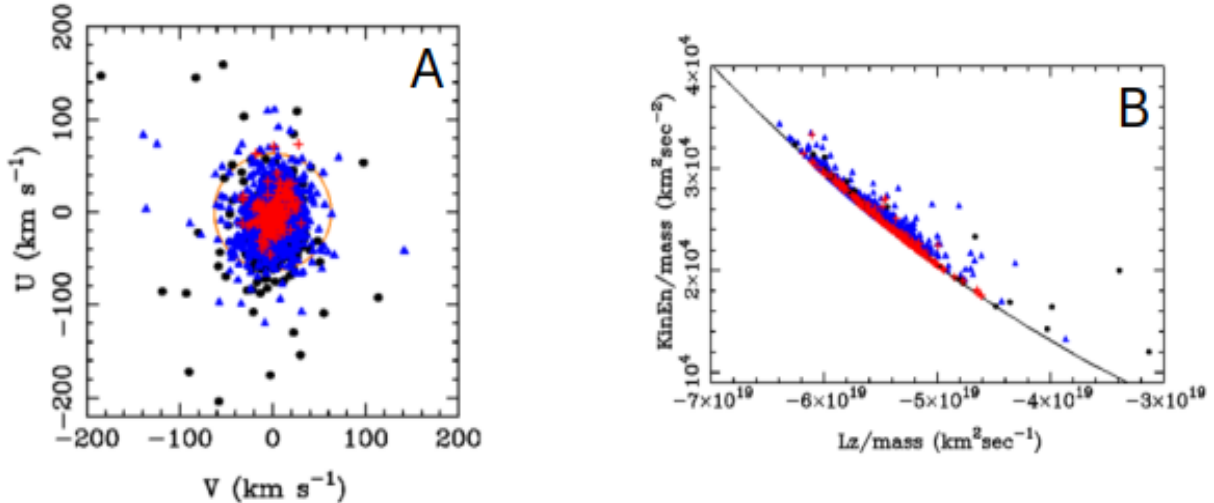


Figure 5. A. Normal dwarfs: A stars (Blue triangles) and B stars (Black filled circles) and peculiar types, ApBp (red crosses) from Houk-Michigan catalogues. The latter form a compact group, almost entirely within the 63 km/s circle, and showing a vertex deviation indicating young objects. B. A striking feature of this KE L_Z diagram is how closely the ApBp stars (red, crosses) cling to the parabola boundary. A few A dwarfs (blue triangles) scatter away from the boundary, and some B dwarfs (black filled circles) scatter somewhat more.

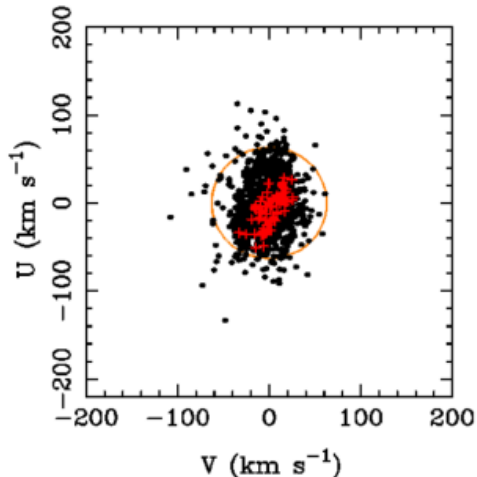


Figure 6. Similar to Fig. 5A but for normal F dwarfs (black filled circles), and AmFm stars (red crosses). The circle is 63 km/s.

In KE vs. L_Z space, 7C, the λ Bootis stars are as closely crowded to the parabola as any stars of our samples.

2.8. G-stars

We have used the BD18 solar twin stars as typical G-stars. However, these 79 stars were chosen from a survey for possible planet hosts (Ramírez et al. 2014). It is therefore useful to compare their properties with the somewhat more numerous (222) G dwarfs of the BSC

(Hoffleit & Saladyga 1997). Kinematic plots are not shown, but Table 1 presents numerical values that show the BD18 and BSC G-stars have quite similar kinematic properties.

3. SUMMARY

The spatial (XY) distributions of Ap, Bp, Am, Fm, and λ Bootis stars fall mostly within a several hundred pc radius of the Sun. The distributions depend on sky coverage and the depth of the relevant surveys as well

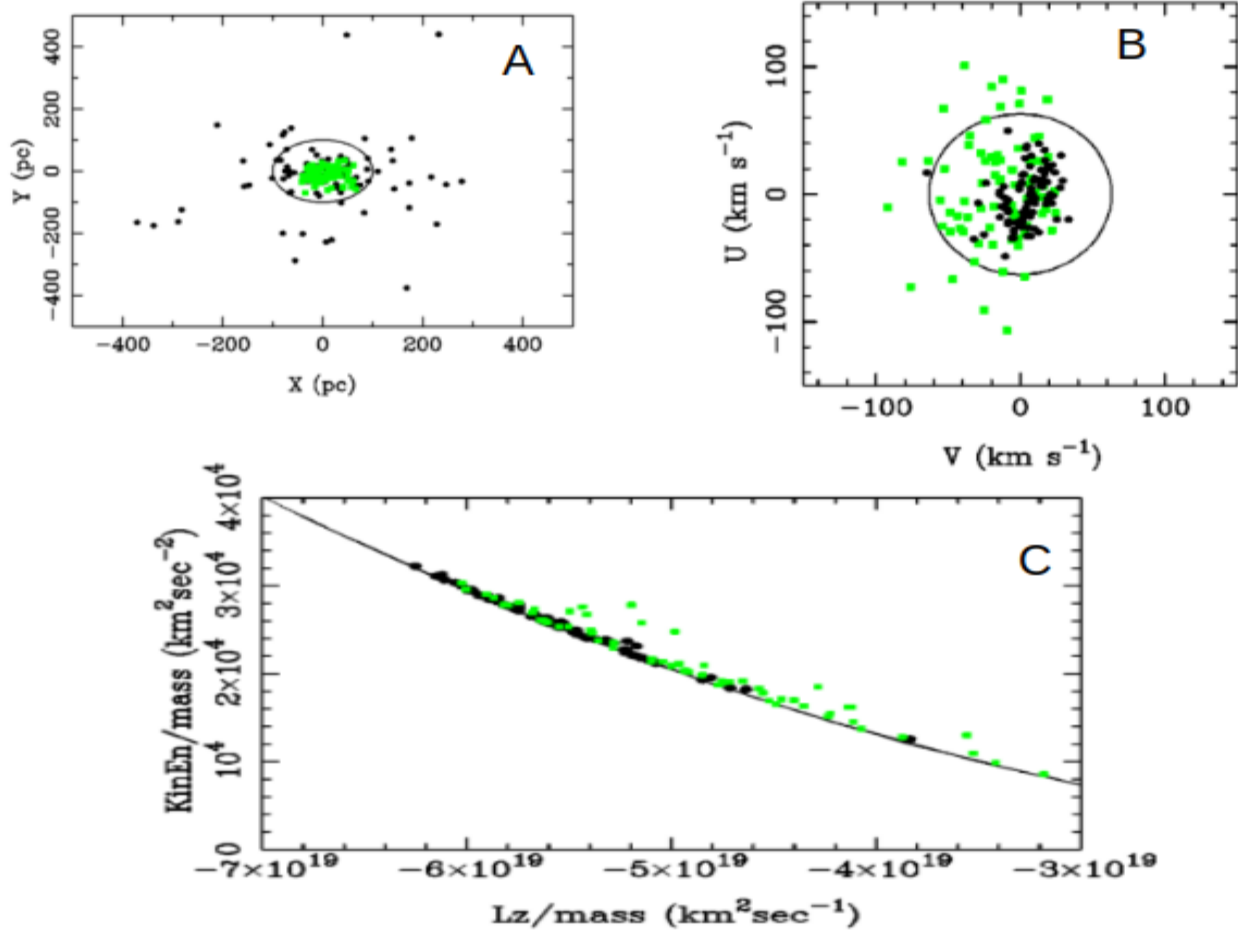


Figure 7. A. The black filled circles are λ Bootis stars, while the green squares are BD18 solar twins. B. λ Bootis stars in velocity space. The black points arguably show a vertex deviation. C. λ Bootis stars in KE vs. LZ space.

as the intrinsic properties of the populations. This is especially clear in the XY plot for the O-stars, where the points scatter beyond 4 kpc because of their high luminosities. The XY plot of the WR stars extends beyond 5 kpc, and has an irregular structure.

The velocity (UV) distributions of the Ap, Bp, Am, Fm, and λ Bootis stars are all similar to chemically normal stars near the Sun. In the KE vs. L_Z plots, these types show a proclivity to fall on the solar parabola. The O-stars show some scatter off the parabola, while the WR types show puzzling L_Z values including retrograde orbits. A summary of relevant numerical values for the various sets of stars is given in the following table, below.

4. DATA AVAILABILITY

The data underlying this article are available in the articles referenced and the Simbad and Gaia data bases.

5. ACKNOWLEDGEMENTS

We are grateful to M. Valluri for clarification of various aspects of Galactic structure and kinematics. P. Crowther kindly provided an ASCII version of his table of WR stars along with distance estimates. S. Hubrig and M. Schöller kindly sent us an ASCII version of the Chojnowski et al. (2020) table of HgMn stars. Thanks are due to J. Fernandez-Trincado and C. Reyl for help with the Galactic potential energy. We note that an anonymous reviewer provided many practical comments. We thank D. Nidever and D. Chojnowski for advice on the reliability of APOGEE radial velocities of WR stars. Thanks also to S. Oey for pointing out ejection as a possible explanation for some extreme velocities of WR stars. The second author is sad to note that the first author recently has been moved into hospice care. We used PyAstronomy, <https://github.com/sczesla/PyAstronomy>.

This work has made use of data from the European Space Agency (ESA) mission Gaia (<https://www>.

Table 1. Stellar Data Sets—Number of stars, data source, mean value of $|Z|$, average KE per unit mass, mean dist from left branch of parabola and standard deviations. Ultra metal-poor stars are added (Cowley & Stencel 2023) to emphasize their extreme KE vs. L_Z space distributions due to high orbital eccentricity and/or lower circular velocities.

Data Set	No. Stars	Source	Mean $ Z $ (pc)	$10^{-3}KE[(km\ s^{-1})]^2$	10^{-18} mean dist
O-stars	354	Maiz Apellaniz et al. (2004)	84 ± 123	27.9 ± 15.7	2.21 ± 4.85
B-stars	62	Houk & Swift (2000)	97 ± 133	24.1 ± 4.16	0.86 ± 2.30
A-stars	2138	"	128 ± 111	25.9 ± 2.61	0.34 ± 0.50
F-stars	2718	"	90 ± 85	24.7 ± 4.09	0.77 ± 3.54
G-stars	222	Hoffleit & Saladyga (1997)	24 ± 32	27.9 ± 0.29	0.36 ± 2.55
BD18	79	Bedell, et al. (2018)	23 ± 17	22.2 ± 5.13	1.28 ± 1.56
Wolf-Rayet	274	Rosslowe & Crowther (2015a)	-30.6 ± 144	34.6 ± 30.8	10.4 ± 1.5
ApBp	143	Houk & Swift (2000)	62 ± 59	24.7 ± 2.88	0.27 ± 0.43
AmFm	79	"	49 ± 36	31.6 ± 1.22	1.17 ± 2.71
HgMn	81	Chojnowski et al. (2020)	62 ± 42	24.1 ± 0.27	0.25 ± 0.71
Herbig AeBe	215	Vioque et al. (2018)	78 ± 67	25.7 ± 6.52	0.86 ± 4.68
λ Boo	90	Murphy et al. (2015)	70 ± 64	25.4 ± 3.21	0.31 ± 0.30
UMetalPoor	299	Roederer et al. (2014)	1447 ± 1703	42.48 ± 39.9	39.89 ± 0.00
UMetalPoor	246	Barklem et al. (2005)	7590 ± 13990	55.4 ± 50.9	50.89 ± 0.00

cosmos.esa.int/gaia), processed by the Gaia Data Processing and Analysis Consortium (DPAC, <https://www.cosmos.esa.int/web/gaia/dpac/consortium>). Funding for the DPAC has been provided by national institutions, in particular the institutions participating in the

Gaia Multilateral Agreement. We also acknowledge use of the SIMBAD database (Wenger et al. 2000) operated at CDS, Strasbourg, France. We are grateful for the support of the Michigan Astronomy Department and help from the LSA Technology Services.

REFERENCES

- Allende Prieto, C. 2010, Chemical Abundances in the Universe: Connecting First Stars to Planets, 265, 304. doi:10.1017/S1743921310000785
- Bailey, J. D., Landstreet, J. D., & Bagnulo, S. 2014, A&A, 561, A147. doi:10.1051/0004-6361/201322853
- Barklem, P. S., Christlieb, N., Beers, T. C., et al. 2005, A&A, 439, 129. doi:10.1051/0004-6361:20052967
- Bedell M., Bean J. L., Meléndez J., et al., 2018, ApJ, 865, 68. doi:10.3847/1538-4357/aad908(BD18)
- Binney, J. & Merrifield, M. 1998, Galactic astronomy, Princeton, NJ, Princeton University Press, 1998. (Princeton series in astrophysics) (see p. 631)
- Castelli, F. & Hubrig, S. 2004, A&A, 421, L1. doi:10.1051/0004-6361:20040164
- Chandrasekhar, S. 1960, New York: Dover, 1960, Enlarged ed. See pp 27-29
- Chojnowski, S. D., Hubrig, S., Hasselquist, S., et al. 2020, MNRAS, 496, 832. doi:10.1093/mnras/staa1527
- Cowley, C. R. & Stencel, R. E. 2023, arXiv:2303.17673. doi:10.48550/arXiv.2303.17673
- Cowley, C. R. & Hubrig, S. 2005, A&A, 432, L21. doi:10.1051/0004-6361:200500013
- Crowther, P. A. 2007, ARA&A, 45, 177. doi:10.1146/annurev.astro.45.051806.110615
- Folsom, C. P., Bagnulo, S., Wade, G. A., et al. 2012, MNRAS, 422, 2072. doi:10.1111/j.1365-2966.2012.20718.x
- GRAVITY Collaboration, Abuter, R., Amorim, A., et al. 2018, A&A, 615, L15. doi:10.1051/0004-6361/201833718
- Ghazaryan, S. & Alecian, G. 2016, MNRAS, 460, 1912. doi:10.1093/mnras/stw911
- Gomez, A. E., Delhaye, J., Grenier, S., et al. 1990, A&A, 236, 95
- Gray, R. O. & Corbally, C. J. 2002, AJ, 124, 989. doi:10.1086/341609
- Gray, R. O. & Corbally, C. 2009, Stellar Spectral Classification by Richard O. Gray and Christopher J. Corbally. Princeton University Press, 2009. ISBN: 978-0-691-12511-4
- Hoffleit, D. & Saladyga, M. 1997, VizieR Online Data Catalog, V/36B

- Houk, N. & Swift, C. 2000, *VizieR Online Data Catalog*, III/214
- Lehmann, C., Murphy, M. T., Liu, F., et al. 2023, *MNRAS*, 521, 148. doi:10.1093/mnras/stad381
- Lodders, K. 2003, *ApJ*, 591, 1220
- Lopez, J. A. & Walsh, J. R. 1983, *MNRAS*, 204, 129. doi:10.1093/mnras/204.1.129
- Maiz Apellaniz, J., Walborn, N. R., Galué, H. Á., et al. 2004, *ApJS*, 151, 103. doi:10.1086/381380
- Meynet, G. & Maeder, A. 2005, *A&A*, 429, 581. doi:10.1051/0004-6361:20047106
- Michaud, G. 1970, *ApJ*, 160, 641. doi:10.1086/150459
- Michaud, G., Alecian, G., & Richer, J. 2015, *Atomic Diffusion in Stars*, *Astronomy and Astrophysics Library*, ISBN 978-3-319-19853-8. Springer International Publishing Switzerland, 2015.. doi:10.1007/978-3-319-19854-5
- Mihalas, D. & Routly, P. M. 1968: San Francisco: W.H. Freeman and Company
- Moreno, E., Pichardo, B., & Schuster, W. J. 2015, *MNRAS*, 451, 705. doi:10.1093/mnras/stv962
- Murphy, S. J., Corbally, C. J., Gray, R. O., et al. 2015, *VizieR Online Data Catalog (other)*, 0190, J/other/PASA/32
- Naik, A. P. & Widmark, A. 2023, arXiv:2307.13398. doi:10.48550/arXiv.2307.13398
- Neugent, K. F. & Massey, P. 2023, *AJ*, 166, 68. doi:10.3847/1538-3881/ace25f
- Oort, J. H. 1930, *BAN*, 5, 189
- Preston, G. W. 1974, *ARA&A*, 12, 257. doi:10.1146/annurev.aa.12.090174.001353
- Plotnikova, A., Carraro, G., Villanova, S., Ortolani, S. 2023 *Ap.J.* 949, 31. doi:10.3847/1538-4357/acc458
- Ramírez, I., Meléndez, J., Bean, J., et al. 2014, *A&A*, 572, A48. doi:10.1051/0004-6361/201424244
- Rate, G. & Crowther, P. A. 2020, *MNRAS*, 493, 1512. doi:10.1093/mnras/stz3614
- Roederer I. U., Preston G. W., Thompson I. B., et al., 2014, *AJ*, 147, 136. doi:10.1088/0004-6256/147/6/136 (RO14)
- Rosslowe, C. K. & Crowther, P. A. 2015, *MNRAS*, 449. doi:10.1093/mnras/stv502
- Rosslowe, C. K. & Crowther, P. A. 2015, *MNRAS*, 449. doi:10.1093/mnras/stv502
- Rustamov, J. N. & Abdulkarimova, A. F. 2023, *Azerbaijani Astronomical Journal*, 18, 24. doi:10.59849/2078-4163.2023.1.24
- Schwarzschild, K. 1907, *Nachrichten von der Gesellschaft der Wissenschaften zu Goettingen, Mathematisch-Physikalische Klasse*, 5, 614
- Sembach, K. R. & Savage, B. D. 1994, *ApJ*, 431, 201. doi:10.1086/174478
- Spina L., Meléndez J., Karakas A. I., et al., 2018, *MNRAS*, 474, 2580. doi:10.1093/mnras/stx2938
- Sun, W., Shen, H., & Liu, X. 2023, *ApJ*, 952, 163. doi:10.3847/1538-4357/acdb58
- van der Hucht, K. A. 2001, *VizieR Online Data Catalog*, III/215
- Venn, K. A. & Lambert, D. L. 1990, *ApJ*, 363, 234. doi:10.1086/169334
- Vioque, M., Oudmaijer, R. D., Baines, D., et al. 2018, *A&A*, 620, A128. doi:10.1051/0004-6361/201832870
- Vysotsky, A. N. 1957, *PASP*, 69, 109. doi:10.1086/127030
- Waters, L. B. F. M. & Waelkens, C. 1998, *ARA&A*, 36, 233. doi:10.1146/annurev.astro.36.1.233
- Wenger M., Ochsenbein F., Egret D., Dubois P., et al., 2000, *A&AS*, 143, 9. doi:10.1051/aas:2000332